High performance 1689-nm quantum well diode lasers

Yupeng Duan (段玉鹏)[1], Tao Lin (林 涛)[2], Cuiluan Wang (王翠鸾)[3], Feng Chong (崇 峰)[3], and Xiaoyu Ma (马骁宇)[3]

[1]*Department of Physics, Northwest University, Xi'an 710069*

[2]*Department of Electronic Engineering, Xi'an University of Technology, Xi'an 710048*

[3]*Institute of Semiconductors, Chinese Academy of Sciences, Beijing 100083*

Received March 19, 2007

1689-nm diode lasers used in medical apparatus have been fabricated and characterized. The lasers had pnpn InP current confinement structure, and the active region consisted of 5 pairs of InGaAs quantum wells and InGaAsP barriers. Stripe width and cavity length of the laser were 1.8 and 300 μm, respectively. After being cavity coated and transistor outline (TO) packaged, the lasers showed high performance in practice. The threshold current was about 13 ± 4 mA, the operation current and the lasing spectrum were about 58 ± 6 mA and 1689 ± 6 nm at 6-mW output power, respectively. Moreover, the maximum output power of the lasers was above 20 mW.

OCIS codes: 140.2020, 140.5960, 160.6000, 260.3060.

Diode lasers, which emit light with wavelength longer than conventional fiber optical communication range of $1.31 - 1.55$ μm, have been developed quickly in recent years due to their applications in remote chemical sensing, pollutant detection, molecular spectroscopy, "eye-safe" illuminators, and medical applications[1−3]. Traditionally, such lasers have been developed in the GaSb-based material system, and the lasers emitting in the wavelength range from 1.7 to 5 μm have been reported[1−5]. While for the mid-infrared lasers which emit wavelength less than 2.2 μm, InP-based InGaAsP and InGaAlAs materials have more advantages than the GaSb-based materials, such as low thermal conductivity, low series resistance, mature epitaxial growth techniques, and well-established fabrication processes[6−9].

In China, Pan *et al.* had reported 1.74-μm distributed feedback lasers for the hydrogen chloride gas monitoring application[10], and 1732-nm lasers for medical application had also been fabricated with InGaAs(P) material[11]. As InGaAs(P) quantum well (QW) has more compressive strain when the lasing wavelength exceeds 1.55 μm, in addition, the high indium content ratio will lead to indium segregation during the QW region growth, the performance and the reliability of the lasers are not as well as that of 1.55 μm lasers used in the fiber communication.

In this paper, we report 1689-nm lasers with the buried QW structure. The laser wafer was grown by low pressure metal organic chemical vapor deposition (MOCVD), and the lasers were fabricated by conventional wet etching method. For the laser chips, the threshold current was about 13 ± 4 mA, and the operation current at 6-mW output power was about 40 ± 3 mA; for the transistor outline (TO) packaging lasers, the operation current was about 58 ± 6 mA, and the lasing spectrum was about 1689 ± 6 nm at 6-mW output power.

The laser structure for this work was grown by a three-step low pressure MOCVD technique. All the growth procedures were carried out in an Aixtron AIX200 system. During the first growth step, a 500-nm-thick silicon-doped InP confinement layer epitaxied on (100) oriented n-InP substrate, then active region with separate confinement heterostructure (SCH) scheme was grown. Five 6-nm-thick compressively strained InGaAs wells were separated by slightly tensile strained (0.3%), 10-nm-thick InGaAsP ($\lambda = 1.5$ μm) barriers. These QWs and barriers were sandwiched between two step-grade SCH layers, which consisted of a 50-nm-thick inner InGaAsP waveguide ($\lambda = 1.3$ μm) and a 70-nm-thick outer InGaAsP ($\lambda = 1.15$ μm) waveguide. After the growth of the upper SCH layers, a 200-nm-thick Zn-doped InP cover layer was grown. Schematic diagram of the first step grown structure is shown in Fig. 1. The crystal quality of the structure was tested by double crystal X-ray diffraction and room temperature photoluminescence (PL). Then, 1.8-μm-wide mesa was formed by wet etching process using a 200-nm-thick SiO_2 layer as a mask. During the second epitaxial stage, a 1.0-μm-thick p-type InP and a 1.0-μm-thick n-type InP layers were selectively grown to bury the mesa stripes. Finally, after removing the SiO_2 mask by hydrofluoric acid, the whole structure

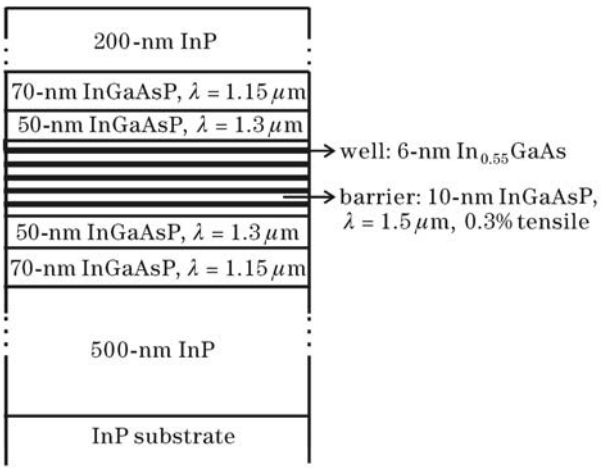

Fig. 1. Schematic diagram of the first step grown structure.

1671-7694/2007/100585-03

was finished by a 2-μm-thick p-InP and a 200-nm-thick p-InGaAs contact layers, and the formed pnpn junctions played current blocking parts for the diode lasers. The whole laser structure was the same as that of the 1732-nm lasers we reported before[11] except for some differences in the active region.

Lasers were fabricated according to a standard procedure. Ohmic contacts were formed with Ti-Pt-Au for the p-side and Au-Ge-Ni for the n-side. Then the wafer was processed into 300-μm-long bars. The front and rear facets were coated anti-reflection (30%) and high-reflection (70%), respectively. The laser chips were mounted junction-side down on copper heat sinks and encapsulated by a standard TO packaging.

Figure 2 shows the X-ray diffraction rocking curve of the laser structure. The main mismatch peaks of the layers are in the range of $\pm$1100 ppm, which are the diffraction peaks of the SCH layers and the QW region. The mismatch of main satellite peak is 580 ppm, and the strong intensities of the satellite peaks demonstrate that the grown active region has high crystal quality and interface morphology. The well agreement between the measurement and the design also indicates the perfect quality of the laser wafer.

Additionally, Fig. 3 shows the room temperature PL spectra of the laser structure. Curve (a) is the PL spectrum of wafer center and curve (b) is the spectrum of the spot 5 mm far from the edge. The peak wavelength of the wafer center is 1693 nm, and that of the spot 5 mm from the edge is 1678 nm. The deviation dispersion of 15 nm over the whole 2-inch wafer is a good result for a long-wavelength laser wafer. Moreover, the full-widths at half-maximum (FWHMs) of the two PL spectra are both 61 nm. The PL measurements reveal that the wafer has good uniformity, and they are also consistent with the results of X-ray diffraction.

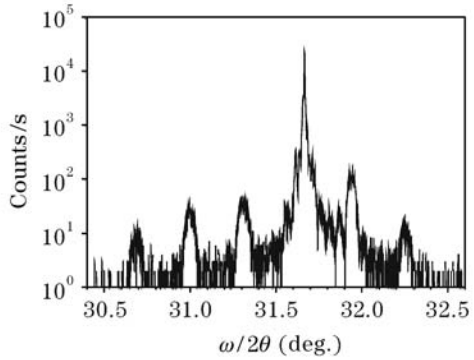

Fig. 2. X-ray diffraction rocking curve of the laser structure.

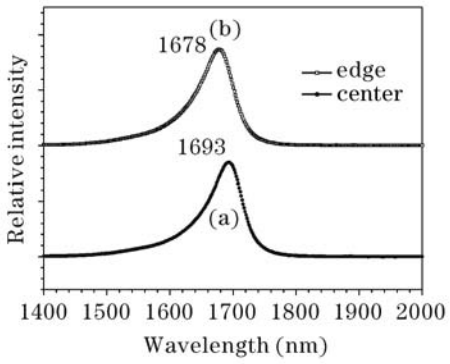

Fig. 3. Room-temperature PL spectra of the laser structure.

In the experiment, we fabricated fifty diode lasers from the same wafer. All these lasers showed a similar performance. Figure 4 shows typical power-current (P-I) and voltage-current (V-I) characteristics of the laser chips and the TO packaging lasers under continuous wave (CW) operation.

For the laser chips, the threshold current is about 13 ± 4 mA, the operation current is 40 ± 3 mA at 6-mW output, and the slope efficiency is about 0.22 ± 0.2 W/A; while for the TO packaging lasers, there is no obvious difference in the threshold current, but the operation current increases to 58 ± 6 mA at 6-mW output, and the slope efficiency reduces to 0.14 ± 0.2 W/A. Two factors may have contributed to the increase in the operation current and the decrease in the slope efficiency between the chips and TO packaging lasers. As we could not provide appropriate pipe caps with anti-reflection coating in 1689-nm waveband for the laser's packaging, pipe caps of standard 1550-nm lasers were used instead, which may be the main reason for the loss of output power. In addition, the light absorption of pipe cap material itself also caused the loss of output power.

Figure 5 shows a typical lasing spectrum of the TO

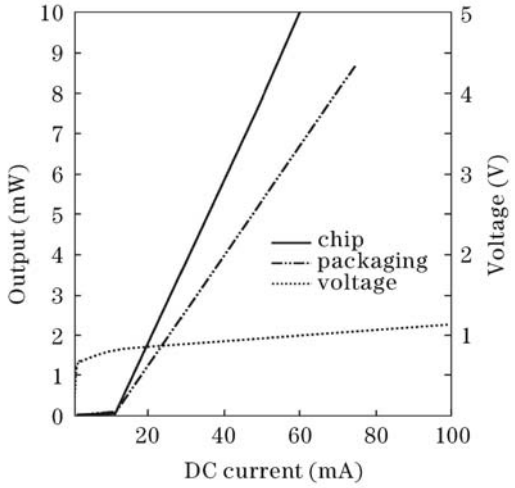

Fig. 4. Typical P-I and V-I characteristics of the laser chips and the TO packaging lasers under CW operation.

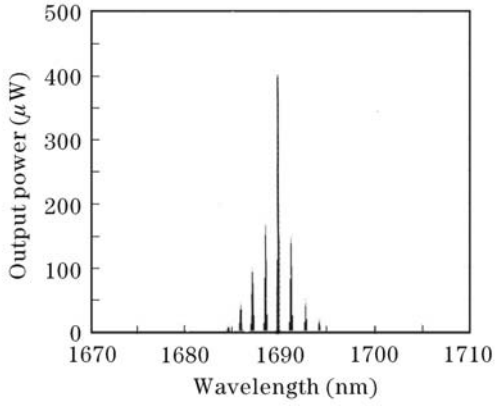

Fig. 5. Typical lasing spectrum of the TO packaging lasers at 6-mW output.

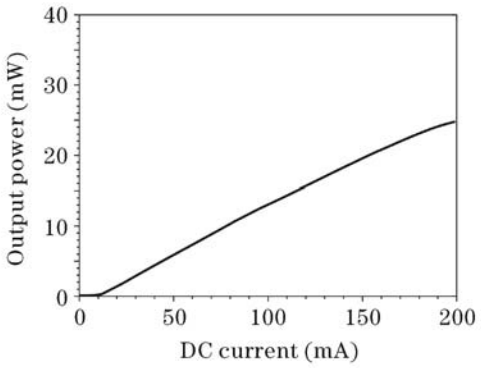

Fig. 6. Typical maximum output power of the TO packaging lasers under CW operation.

packaging lasers at 6-mW output. As shown in the figure, the emitted wavelength is near 1689 nm, and the FWHM of spectrum is 1 nm. In this work, all the lasers emit wavelength in the range of 1689 ± 6 nm, and the FWHMs of spectra are less than 5 nm.

A typical maximum output power of the TO packaging lasers under CW operation is shown in Fig. 6. It can be seen that the maximum CW output power of the 1.8-μm-wide laser is above 20 mW. As the maximum drive current in the test system is 200 mA, the maximum power of the laser will be higher before a thermal saturation or device failure happens.

Long-term reliability is a critical factor for lasers used in medical apparatus, so the useful lifetime of the 1689-nm laser which has large compressive strain InGaAs QWs was tested. In accordance with the Bellcore standard, we defined the screening test conditions of 90 °C, 100 mA, and 24 h. After the high-temperature constant-current accelerating aging test, none of the fifty TO packaging lasers failed and the increases in the threshold current and operation current were both below 2%. Results of the burn-in screening test show that the lasers are reliable for long-time working and can meet the practical application.

In conclusion, high performance 1689-nm QW laser diodes have been fabricated. The laser structure was grown by a three-step low pressure MOCVD technique. The TO packaging lasers show threshold current of about 13 ± 4 mA, operation current of 58 ± 6 mA, and lasing spectrum of 1689 ± 6 nm at the output power of 6 mW. Moreover, the maximum output power of the lasers is over 20 mW, and all the lasers show high reliability after accelerating aging test. These results show that the lasers have high performance of practical use and can be used as laser sources in medical instruments.

The authors gratefully acknowledge Guangze Zhang, Kai Zheng, Suping Liu for their supports in the material growth and devices testing. Y. Duan's e-mail address is yupengduan@sina.com.

References

1. H. K. Choi, G. W. Turner, M. K. Connors, S. Fox, C. Dauga, and M. Dagenais, IEEE Photon. Technol. Lett. **7,** 281 (1995).
2. D. Z. Garbuzov, H. Lee, V. Khalfin, R. Martinelli, J. C. Connolly, and G. L. Belenky, IEEE Photon. Technol. Lett. **11,** 794 (1999).
3. R. Werner, T. Bleuel, J. Hofmann, M. Brockhaus, and A. Forchel, IEEE Photon. Technol. Lett. **12,** 966 (2000).
4. M. Garcia, A. Salhi, A. Pérona, Y. Rouillard, C. Sirtori, X. Marcadet, and C. Alibert, IEEE Photon. Technol. Lett. **16,** 1253 (2004).
5. G. L. Belenky, J. G. Kim, L. Shterengas, A. Gourevitch, and R. U. Martinelli, Electron. Lett. **40,** 737 (2004).
6. J.-S. Wang, H.-H. Lin, and L.-W. Sung, IEEE J. Quantum Electron. **34,** 1959 (1998).
7. G. K. Kuang, G. Böhm, M. Grau, G. Rösel, R. Meyer, and M.-C. Amann, Appl. Phys. Lett. **77,** 1091 (2000).
8. G. K. Kuang, G. Böhm, N. Graf, M. Grau, G. Rösel, R. Meyer, and M.-C. Amann, IEEE Photon. Technol. Lett. **13,** 275 (2001).
9. D. Wang, N. Zhou, J. Zhang, Y. Liu, N. Zhu, and L. Li, Chin. Opt. Lett. **3,** 466 (2005).
10. J. Pan, W. Wei, H. Zhu, Q. Zhao, B. Wang, F. Zhou, and L. Wang, Chin. J. Semiconductors (in Chinese) **26,** 1688 (2005).
11. T. Lin, K. Zheng, C. L. Wang, J. Wang, Y. Wang, L. Zhong, X. Feng, and X. Ma, Chin. J. Semiconductors (in Chinese) **27,** 1467 (2006).